MSc thesis

Aquifer storage and recovery in a fossil creek bed

managing droughts in a brackish environment

Martijn Visser, August 23, 2012

Programme Hydrology, track Environmental Hydrogeology
Supervisors Esther van Baaren (Deltares)
Pieter Pauw (Deltares)
Prof. Dr. Ruud Schotting (Utrecht University)

Abstract

In the Dutch coastal province of Zeeland, there is a lack of freshwater that can be used for irrigation during dry spells in May–August. A promising solution may lie in a geological feature of the region. There are sandy fossil creek beds that, after the surrounding marshland subsided, became elevated in the area. The permeable sand provides good conditions for the growth of freshwater lenses. The goal of the research is to find effective ways to increase the thickness of the lens, such that it can be used to sustainably pump freshwater from this reservoir in times of drought.

On a creek ridge north of Serooskerke, Walcheren, electrical conductivity measurements were done using several different geophysical methods. This showed freshwater lenses of around fourteen metre thick. The area was then modelled in a 3-D density dependent groundwater flow model with coupled salt transport, using the code MOCDENS3D. Model results showed that there are currently two main factors limiting freshwater lens growth. Firstly, there is a primary ditch cutting deep through the sandy creek. Fresh groundwater flows from the creek bed into the brackish ditch. Also, if the current conventional drainage on the sandy creek were to be replaced by controlled drainage, unnecessary drainage could be prevented. Whilst eliminating these two points would already thicken the freshwater lens by a few metres, further success could be made by artificially infiltrating extra freshwater into the creek ridge. This can be done through the controlled drainage, during winter months when surplus freshwater is available. Artificially infiltrating extra water could help balance for the water that is pumped out of the creek ridge in summer, to prevent upconing of brackish water.

Deltares
Enabling Delta Life

Universiteit Utrecht

Contents

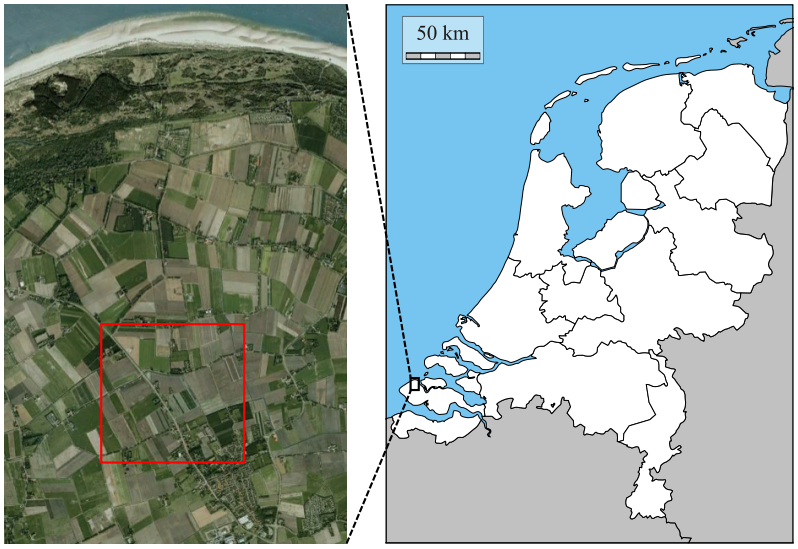

Figure 1: Location of the area in the Netherlands. The red box is the modelling domain, 1600 × 1600 metres. Image credit: Google Earth, Daniel Dalet / d-maps.com

1 Introduction

In the Dutch province of Zeeland, in the farmlands between Serooskerke and Oostkapelle, freshwater is a scarce and valuable commodity during the summer months. The area, shown in Figure 1, is characterised by surface levels around NAP (*Nieuw Amsterdams Peil*; the Dutch national ordinance level, approximately equal to mean sea level). The North Sea is 3 km away, the land is protected from it by dunes and dikes. As a result of the low land elevation, the area deals with saline seepage into the ditches, and generally thin rainwater lenses on top. Local farmers want to irrigate their crops during dry spells in May–August. However due to the saline seepage the surface water is often too salty to use. No irrigation during dry spells can result in a large fraction of the crop suffering from drought damage. This work seeks an innovative approach to alleviate these fresh-salt groundwater problems.

The research was carried out at Deltares in Utrecht. Deltares is involved in this work as a part of the Waterhouderij concept. This concept is developed by Aequator as commissioned by InnovatieNetwerk and TransForum. The Waterhouderij is envisioned as a cooperation between local farmers, municipalities, water boards and inhabitants with the goal to work together to manage and store the excess winter freshwater more effectively, such that the area does not depend on external freshwater supply. In Walcheren, in the triangle between the villages of Oostkapelle, Serooskerke and Vrouwenpolder such a cooperation has been established in July 2011, named Waterhouderij Walcheren. It functions as a pilot area for the applicability of the Waterhouderij concept.

Before men started living in Walcheren, it was an intertidal area. There was a lot of peat in the landscape. Tidal channels easily cut their way through the peat. Through these tidal channels the tides came in. Water velocities were high such that only sand would form the bed for these channels. When the tidal flats flooded, water velocities reduced such that smaller particles like clay could be deposited on top of the existing peat. Since the reclamation of the land, the peat and clay have subsided, causing the

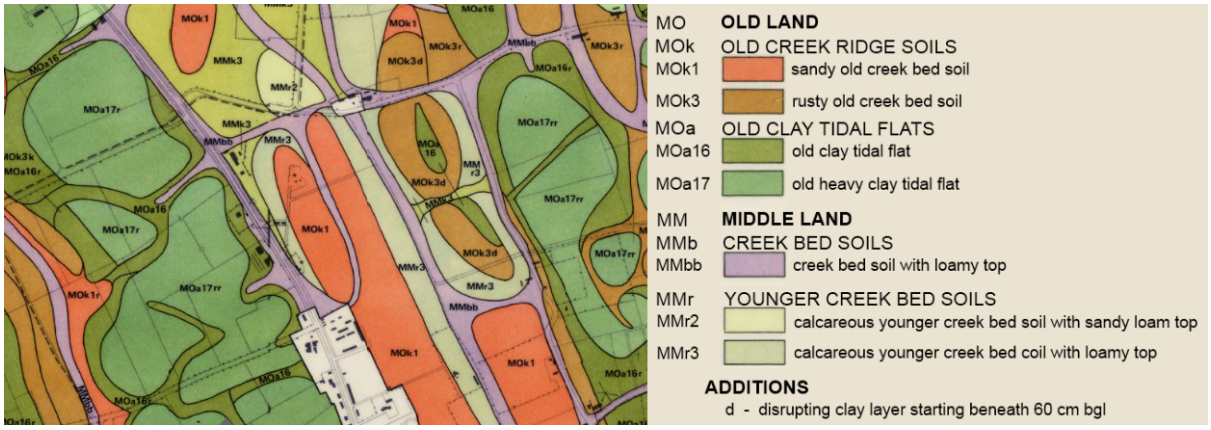

Figure 2: Detailed soil map of the area, showing the sandy creek ridge surrounded by reclaimed tidal marshes. After [*van Betuw*, 1952].

sandy fossil creek beds to become elevated in the landscape, hence the name creek ridge.

Just north of Serooskerke, Walcheren, there is a typical creek ridge. It can be recognized from the soil type, Figure 2, and from the elevation map, Figure 3. Two farmers that participate in the Waterhouderij Walcheren project have their agricultural land on this ridge. Their names are Johan Sanderse and Werner Louwerse, and their main crops are respectively potatoes and cauliflower or fennel. Their land on the creek ridge will be the main area of interest in this work. This is because creek ridges are known to have relatively large fresh groundwater lenses. This makes for an interesting freshwater reservoir, that, as opposed to building a freshwater basin, is free. To be able to pump water sustainably the lens has to be properly supplied with enough fresh water during times of excess. Finding ways to achieve this is the goal of this research. If the research succeeds in finding possibilities to increase freshwater supply in the creek ridge, these methods can be considered for other farmers on creek ridges found throughout Zeeland.

A pilot study to field-test the effectiveness of artificial infiltration to increase the freshwater lens at this location have been proposed as part of the *Knowledge for Climate* research programme [*Stuyfzand*, 2010]. This has since been accepted and will start in the winter of 2012/2013, such that in the near future field data will complement the modelling results described in this work.

2 Research questions

- How can the freshwater supply from the creek ridge north of Serooskerke, Walcheren be increased?
  - What geophysical measurements are necessary for the main research question to be answered adequately?
  - How does the hydrogeological system on the sandy creek ridge work?
  - Is injection of freshwater through a controlled drainage system an effective way to increase the freshwater lens?
  - Are there any other sustainable ways to increase the freshwater lens?

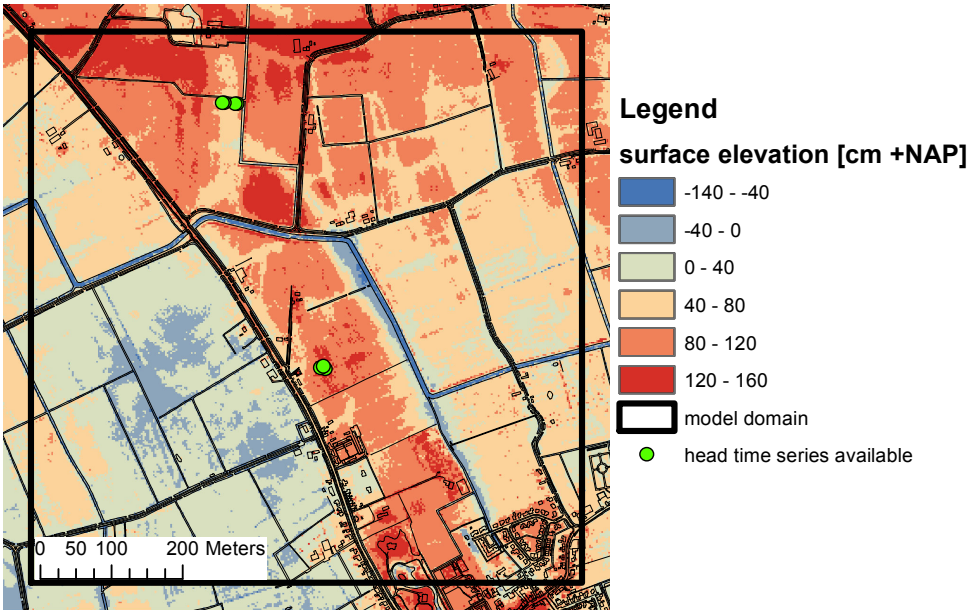

Figure 3: Surface elevation map. The chosen model domain is also indicated.

3 Literature review

Aquifer storage and recovery (ASR) is a well known concept with many studies. However the specific goals and means that ASR is used for in this research is almost undocumented. ASR is commonly associated with well injection into confined aquifers [*Pyne*, 2005]. In this case however ASR will be done in a heterogeneous phreatic aquifer, where saline groundwater is present at relatively shallow depth. Naturally a part of the water injected into this system is lost. Therefore the term LSR-ASR, Leaky Storage Reservoir combined with phreatic Aquifer Storage and Recovery via the reservoir, has recently been coined for this new technology [*Stuyfzand*, 2010]. The reservoir size in this work is small, for it concerns seasonal storage on a single plot of land. The objectives of this LSR-ASR is both agricultural water supply and preventing salt water intrusion [*Stuyfzand and Doomen*, 2004]. The means of infiltration will be a controlled drainage system. This system can be used for infiltration and has been successfully used for this purpose according to experiences of farmers. Currently there is another field experiment going on in the Dutch province of Noord-Brabant where they look at infiltrating water through controlled drainage. However because of the location they need not worry about salt water intrusion, which is a very important part of this research.

There have been previous attempts at injecting freshwater in creek ridges. These have been done in the Netherlands in the 80s [*van Meerten*, 1986]. While certainly useful as a reference in this study, they are also much simplified, using for instance the Ghyben-Herzberg stationary interface in their model [*van der Straat*, 1986]. In the Ghyben-Herzberg model the depth of the interface below sea level can be calculated as forty times the water table elevation above sea level. No mixing at the interface is assumed and the interface depth is determined solely by the density gradient, the buoyancy of freshwater over saline water. Recent work by de Louw [2011] on shallow rainwater lenses shows that in saline seepage areas the location of the fresh-salt interface is mostly determined by

head gradients (forced convection) rather than density gradients (free convection). It is expected that this is also true for the creek ridges discussed in this work, because they lie in a general saline seepage area. Whilst the surface elevation of the creek ridge lies above NAP, the groundwater table generally does not. It is surrounded by low lying ditches that attract saline seepage. This upward flow of saline groundwater likely limits the development of the rainwater lens on the creek bed much like described by de Louw. For these reasons the Ghyben-Herzberg relation is not appropriate for this research.

Outside of the Netherlands research concerning freshwater lenses seems to be more focused on lenses on the scale of kilometres wide [*Panday et al.*, 1993], [*Sanford and Pope*, 2010]. Although not unique, the Dutch situation where coastal farmlands below mean sea level, experiencing saline seepage, are relying on plot-wide rainwater lenses is not common in the world.

The modelling part of this research was done using the numerical code MOCDENS3D by Oude Essink [2001]. This code has been used before to make a regional density dependent groundwater model of Zeeland, with grid cells of $100 \times 100\ m^2$ [*van Baaren et al.*, 2012]. Since this model is regional and the one to be developed in this research is much more local, the resolution will be increased to $10 \times 10\ m^2$.

4 Theory

The density of water varies with both temperature and chemical composition. In a fresh groundwater model with normal groundwater temperatures of around 10 °C, density variations are usually considered negligible and it is taken as a constant of $1000\,\mathrm{kg/m^3}$. This simplification cannot be made for this model as the density varies between $1000\,\mathrm{kg/m^3}$ for freshwater and $1025\,\mathrm{kg/m^3}$ for seawater. This is due to salts dissolved in the water. Sodium chloride takes up the largest part of the dissolved salts, such that in this model only the chloride concentration is considered and directly related to the water density. Since in this model temperature variations do not play a significant role, variable density is implemented to be linearly dependent on the chloride concentration, giving the equation of state:

$$\rho(C) = \rho_f \left(1 + \alpha \frac{C}{C_s}\right)$$

where $C_s = 18630 mg\ Cl^-/l$ is the chloride concentration of seawater, $\rho_f = 1000\,\mathrm{kg/m^3}$ the density of freshwater, and $\alpha = (\rho_s - \rho_f)/\rho_f = 0.025\,[-]$ the relative density difference. All computed concentrations will be presented as chloride concentrations $[mg\ Cl^-/l]$; Table 1 is used to classify the type of groundwater. When the fresh-salt interface depth is mentioned in this work, it generally refers to the depth of groundwater with a concentration of $1000 mg\ Cl^-/l$, a commonly used value in Zeeland.

The value of the hydraulic conductivity K depends on both the porous medium and the water, defined as follows:

$$K = \frac{\kappa \rho g}{\mu} \tag{1}$$

where κ is intrinsic permeability of the porous medium [$\mathrm{m^2}$], μ is dynamic viscosity [kg/(m s)] and g is acceleration due to gravity [$\mathrm{m^2/s}$]. Technically, the value of K should vary through salinity effects on both density and dynamic viscosity in (1). However

Table 1: Classification of types of groundwater based on chloride concentration. After Stuyfzand [1986].

Type of groundwater	Chloride concentration $[mg\ Cl^-/l]$		
fresh		$<$	150
fresh-brackish	150	–	300
brackish	300	–	1000
brackish-saline	1000	–	10 000
saline	10 000	–	20 000
hypersaline or brine	20 000	$<$	

typical dynamic viscosity variations are minor and it can be approximated to be constant (Verruijt, 1980; Bear & Verruijt, 1987 in [*Oude Essink*, 1999]). Hydraulic conductivity for saline water can be at most $(\rho_s - \rho_f)/\rho_f = 2.5\%$ higher compared to freshwater. This falls well within the uncertainty of K determination, and for this reason no distinction is made between conductivity K and freshwater conductivity K_f, which has a fixed density ρ_f.

For constant density situations the hydraulic head is normally used to model groundwater flow. The head is relatively easy to measure, and can be directly inserted into Darcy's law, $\mathbf{q} = -\mathbf{K}\nabla h$, to calculate flow. Hydraulic head consists of the sum of pressure head and elevation head, $h = \psi + z = (P/\rho g) + z$, where P is gauge pressure [Pa]; g is acceleration due to gravity [m^2/s] and z is the elevation at the piezometer bottom [m]. The head is thus dependent on the density. In the field this means that fresh water will rise higher in a piezometer compared to saline water, even though the pressure is equal at the bottom. In this scenario one can use the density in the piezometer to calculate the pressure P and use that to model variable density groundwater flow.

However most hydrologists are used to modelling heads instead of pressures, and find it a more intuitive unit. An alternative solution is to use the fictional *equivalent freshwater head*, h_f, which is the head that would be measured if the piezometer would be filled with fresh water [*Post et al.*, 2007]. It is defined as follows:

$$h_f = \frac{P}{\rho_f g} + z \tag{2}$$

such that the density is fixed to that of freshwater. Measured heads in the field can be converted to equivalent freshwater heads, such that they can be compared to one another. Since MOCDENS3D is based on freshwater heads, Darcy's law needs to be rewritten in terms of freshwater head. This is first done for the horizontal x and y directions. In the last step (2) is solved for P and then differentiated. Note also that since in this work $K_x = K_y \neq K_z$ the terms K_h and K_v are used for respectively horizontal and vertical conductivities.

$$q_x = -K_h \frac{\partial h}{\partial x} = -K_h \frac{\partial}{\partial x}\left(\frac{P}{\rho g} + z\right) = -\frac{K_h}{\rho g}\frac{\partial P}{\partial x} = -K_h \frac{\rho_f}{\rho}\frac{\partial h_f}{\partial x} = -K_{f,h}\frac{\partial h_f}{\partial x} \tag{3}$$

$$q_y = -K_h \frac{\partial h}{\partial y} = -K_h \frac{\partial}{\partial y}\left(\frac{P}{\rho g} + z\right) = -\frac{K_h}{\rho g}\frac{\partial P}{\partial y} = -K_h \frac{\rho_f}{\rho}\frac{\partial h_f}{\partial y} = -K_{f,h}\frac{\partial h_f}{\partial y} \tag{4}$$

From this it can be concluded that variable density does not influence the horizontal flow components, as head can be freely interchanged with freshwater head. For the vertical

flow component the derivative of the elevation head does not equal zero, leaving an extra term:

$$q_z = -K_v \frac{\partial h}{\partial z} = -K_v \frac{\partial}{\partial z}\left(\frac{P}{\rho g} + z\right) = -K_v \left(\frac{1}{\rho g}\frac{\partial P}{\partial z} + 1\right) = -K_{f,v}\left(\frac{\partial h_f}{\partial z} + \frac{\rho - \rho_f}{\rho_f}\right) \tag{5}$$

the extra term, $(\rho - \rho_f)/\rho_f$, is a buoyancy term, and is responsible for the formation of freshwater lenses, where freshwater is buoyant over saline water.

Chloride is a conservative solute. This means that it does not react with other matter, and it does not adsorb or decay. The chloride ions stay dissolved in the water, and move at the same speed as the water molecules. Since adsorption and decay do not need to be considered for chloride transport, the only transport mechanisms that are modelled are advection, diffusion and dispersion. For only the x-direction this is given by the following partial differential equation:

$$\frac{\partial C}{\partial t} = D_x \frac{\partial^2 C}{\partial x^2} - \frac{q_x}{n}\frac{\partial C}{\partial x} \tag{6}$$

where C is chloride concentration; D is the hydrodynamic dispersion coefficient; q is Darcy flux and n is the porosity.

5 Fieldwork

In December of 2011 a fieldwork campaign was done on location. The purpose of the measurements was twofold: firstly field data is essential to calibrate and verify the model, and secondly the measurements will jointly form a good picture of the current state of the freshwater lens. After the planned field tests to increase the freshwater lens have been performed, the new measurement results can be compared against the presented initial measurements to examine the effectiveness of the tests. The CVES measurements were performed by Pauw, most other data was collected and processed by the author. Short descriptions of the equipment and how they work is also provided.

5.1 TEC probe

A temperature-electrical conductivity (TEC) probe is a probe that is manually pushed into the ground, up to 4 m deep. It has a tip with a temperature sensor, and right above this are two electrodes that measure the apparent conductivity in the saturated subsoil. Starting from the groundwater table, every 10 cm a reading was done until the probe could not be pushed any further. This was the case when a layer with high sand content was hit. Since the fossil creek bed is sandy, TEC probing was only successful close to the edge of the fossil creek with the primary ditch, where the subsoil is rich in clay.

As mentioned the *apparent* conductivity is measured in the saturated subsoil. This conductivity is a combination of the conductivity of the groundwater and the subsoil. The material of the subsoil affects the conductivity, and for the groundwater the conductivity increases with the presence of free ions in the water. The major part of the free ions in the water are sodium and chloride ions. To isolate the effect of groundwater salinity

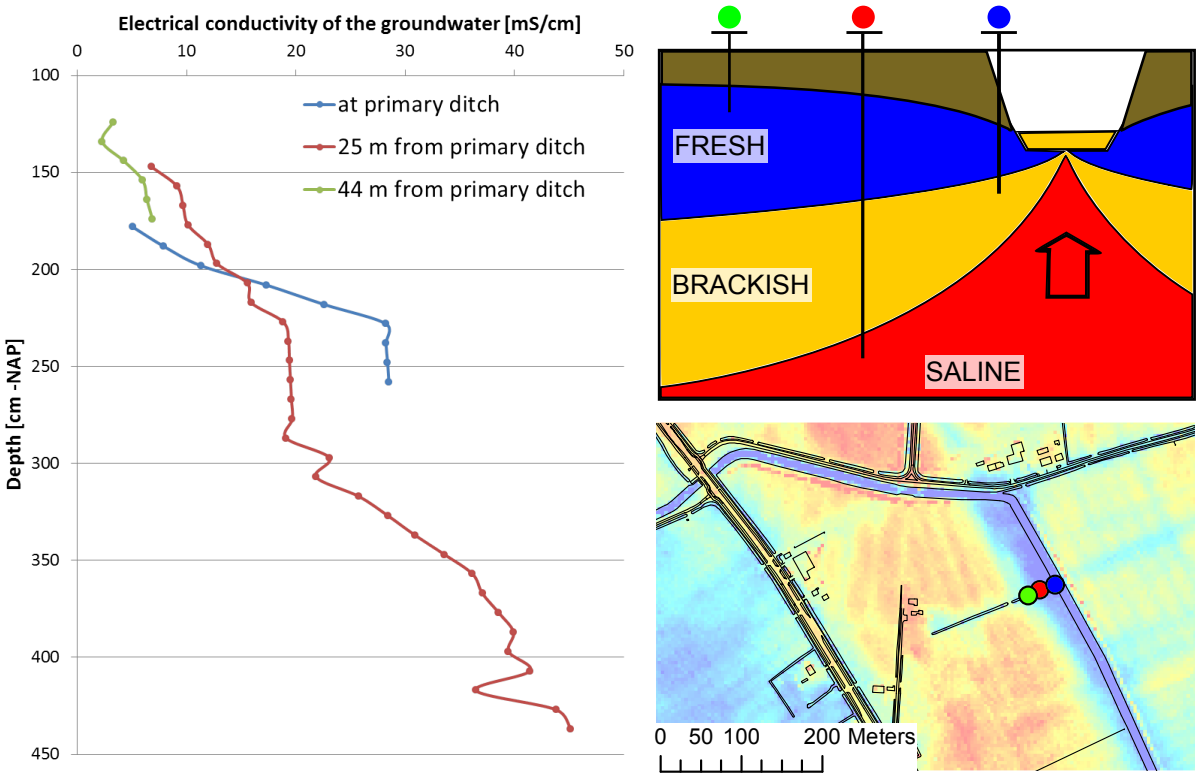

Figure 4: Left: three profiles of electrical conductivity of the groundwater, showing an increase in the salinity at greater depths. Right top: conceptual image supported by the TEC probe measurements. Right bottom: location of probing locations as indicated by the coloured circles. Background color indicates relative surface elevation to show location of the creek ridge.

on the apparent conductivity, tabulated formation factors from de Louw [2011] are used. These factors were determined in the field in Zeeland.

The three electrical conductivity depth profiles done with the TEC probe are shown in Figure 4. All three are along a line of 44 m, perpendicular to the direction of the sandy creek. The highest data points are all 30 cm below water level, such that the ridge-side of the line lies 50 cm higher. Since probing is the easiest in clay-rich sediment, the profile was made in a small drainage ditch over the creek ridge. As will be shown in the CVES measurements, this small ditch causes only slight upconing, but no saline seepage into the ditch. This does not happen because the elevation of this ditch follows the profile of the ridge, and thus lies higher than the primary ditch in which it ends.

The deepest profile, coloured red in Figure 4, shows a depth profile of three metres. Over the complete profile the conductivity increases, though less so at the deepest point, suggesting a fresh-salt interface of around three metres thick. The green coloured profile, the furthest towards the ridge, shows freshwater on top, but does not go deep enough to show the interface. Right at the edge of the primary ditch the blue coloured profile was taken. Already 30 cm below the completely fresh ditch drainage water a quickly rising conductivity is observed. Although the conductivity stays constant at the deepest point of the profile, it is believed it will rise further. At the same depth in the red coloured profile 25 m away, this constant conductivity also occurs. This could be explained by a more permeable layer which is well mixed vertically.

Figure 5: GEONICS EM31 as it is used in the field. Image credit: FPM Geophysical & UXO Services.

5.2 GEONICS EM31

Whilst using a TEC probe can generate nice depth profiles, it is not easy to form an idea of the lateral extent of the freshwater lens. The GEONICS EM31 measures the bulk apparent conductivity of, effectively, the top 6 m of the subsurface. The device, pictured in Figure 5, consists of a four metre long boom with a transmitting coil on one end and a receiving coil on the other end. The device uses an active frequency domain electromagnetic technique, meaning that an alternating current is applied to the transmitting coil. This creates a primary electromagnetic field that penetrates the ground. This field induces eddy currents, especially so in high conductivity regions, which are responsible for a secondary electromagnetic field, which in turn is picked up by the receiving coil. Combining measured strength of the primary and secondary electromagnetic field, the apparent conductivity is automatically calculated. Whilst for the TEC probe measurements formation factors were used to remove effect of variable subsurface materials on the conductivity, this was not done for the EM31 measurements, since there is no appropriate formation data available. In the field the EM31 was combined with a GPS unit, allowing georeferencing of the data.

A total distance of circa 6 km was traversed, mostly along and across the fossil creek bed, to map out the horizontal extent of the freshwater lens. Figure 6 shows the georeferenced apparent electrical conductivity readings. The effect of the salinity of groundwater is expected to be dominant over the effect of soil type on the electrical conductivity. However one can compare the results with the soil map of Figure 2. Around the middle of the creek ridge, the EM31 electrical conductivity readings are the lowest. It is very likely that in these dark blue coloured regions the fresh-salt interface begins below six metres depth, below the reach of the EM31. In paths crossing over the ridge towards the primary ditch, the conductivity increases until the primary ditch, where it is known from the TEC measurements that the freshwater lens is very thin. The EM31 measurements correlate closely with the surface elevation. The outcome of these measurements was as expected, though now it is confirmed that the lens does occur along the entire length of (this section of) the creek ridge.

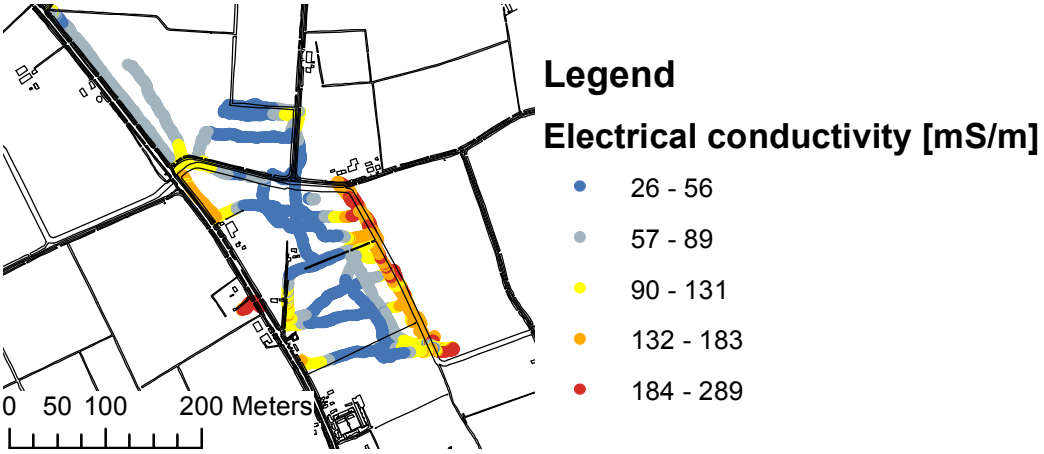

Figure 6: Apparent electrical conductivity of the top 6 m of the subsoil, as measure by the GEONICS EM31. Whilst varying subsurface materials also affect the readings, a general pattern of a freshwater lens along the length of the sandy creek ridge can be seen.

5.3 CVES

Since the freshwater lens is thicker than the penetration depth of the EM31, another technique is used to create cross-sections of the complete freshwater lens. Continuous Vertical Electrical Sounding (CVES) is done by inserting an array of electrodes into the top soil along the cross-section, and connecting them to a central unit. A current is sent between two electrodes, and at the same time another pair of electrodes measure the potential difference. After this is done for many combinations of electrodes, inversion software can be used to produce resistivity maps [*Pauw*, 2011]. A photo showing the device in the field can be seen in Figure 7. A total of four transects were done, their locations are presented in Figure 8. Figures 9–12 show the results of the four transects, with a discussion in the caption.

5.4 Groundwater table fluctuations

In 2011 shallow piezometers were installed on two different locations, as indicated in Figure 3 on page 5. These piezometers were equipped with divers, which measure the water pressure hourly. This was combined with air pressure data and elevation data, to create two groundwater level time series. The result can be seen in Figure 13. Heads are plotted with respect to NAP, but for reference, the surface elevations at the two locations are 1.4 m +NAP and 0.5 m +NAP for respectively the creek and the north location. During the dry spring of 2011 the groundwater table dropped in the North by 0.5 m. Winter recharge came late, but during an unusually wet week in December (when the author was doing the fieldwork) the groundwater level sore up by a metre. A large part of this is drained away over the course of another week. The piezometer on the creek is placed by the horizontal well of the farmer. A small pumping test was performed in August 2011, and the pump was again used in March 2012, when an estimated 330 m^3 was pumped out at a rate of 4 m^3/hour. Whilst drawdown in the immediate vicinity is large, the groundwater table can be seen to return quickly to original levels.

Figure 7: CVES equipment in the field in Walcheren. Electrodes are pushed into the ground every metre along the transect, and are controlled automatically by a unit seen in the distance.

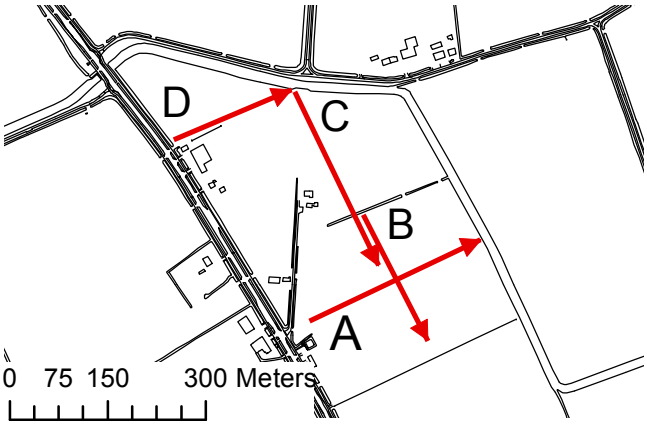

Figure 8: Locations of the four transects. Arrows indicate positive x-axis direction in Figures 9–12.

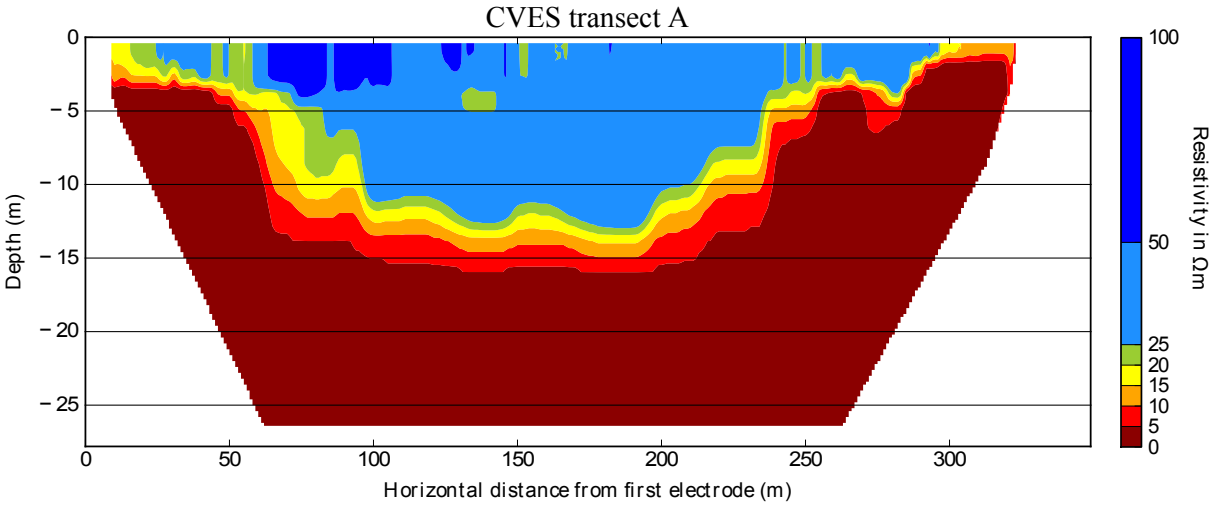

Figure 9: Transect A is across the creek ridge. The fresh-salt interface is around 5 m thick, and in the middle, at the highest point of the ridge the freshwater lens reaches a maximum thickness of 14 m.

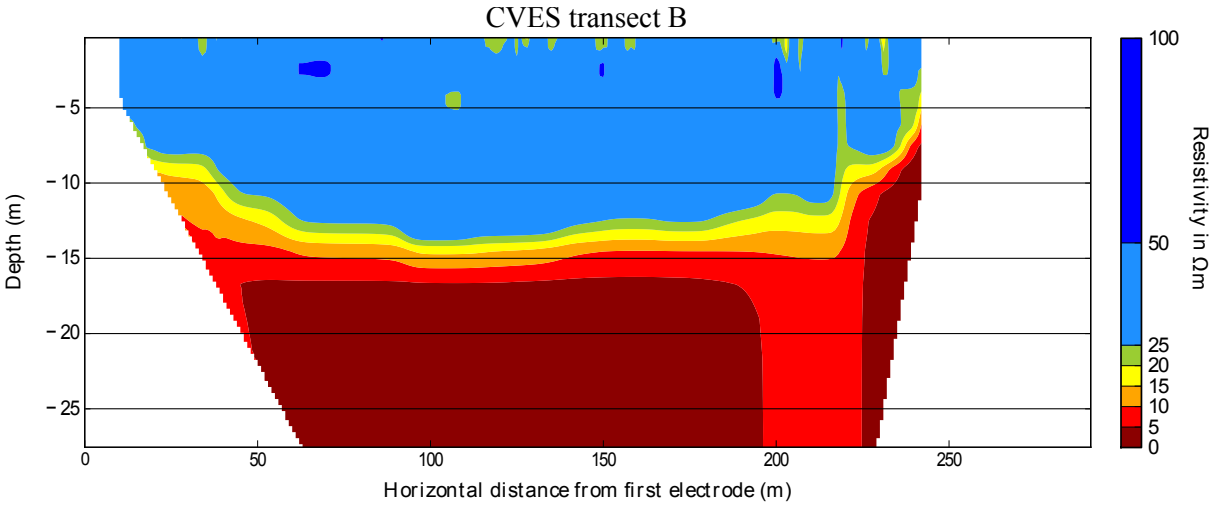

Figure 10: Transect B is along the middle of the sandy creek ridge. There is visible upconing on both ends of the profile. On the left side this is caused by the small drainage ditch that goes across the ridge. On the right side there is strong upconing. The farmer commented that there are two old drainage pipes buried at 2 m depth, 1 m deeper than the other drainage pipes. These drains run across the ridge at the location of this upconing and are known to transport large amounts of water towards the primary ditch, so the upconing is thought to be a result of these two drainage pipes.

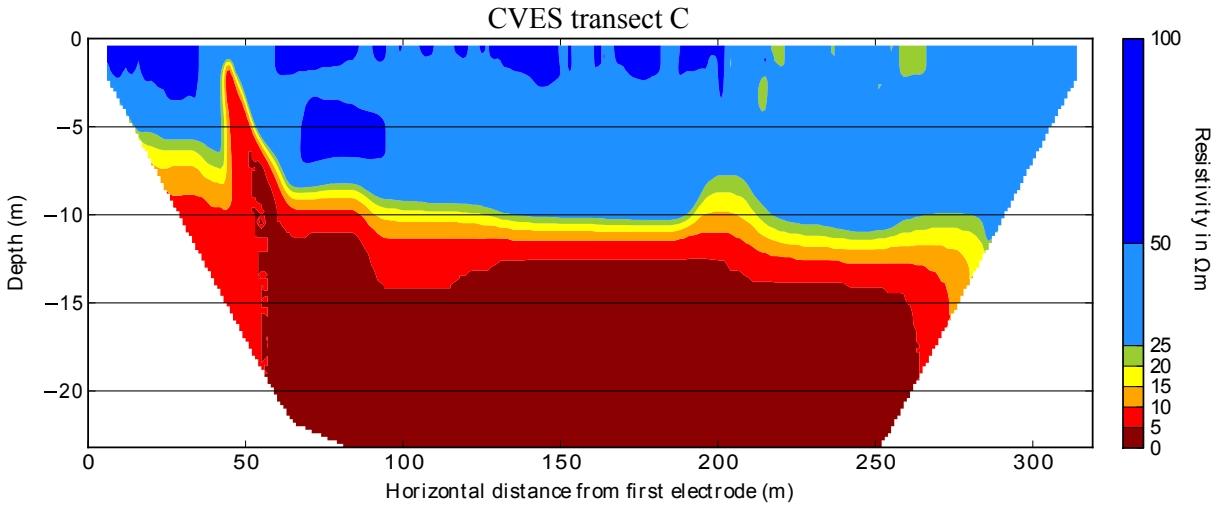

Figure 11: Transect C is, like transect B, along the creek ridge. However this one starts where the primary ditch cuts through the sandy creek. The high peak around $x = 50$m is an artefact caused by a buried cable and should be ignored. On the left half there is a steadily thinning freshwater lens. A 5 m thick lens remains close to the primary ditch, because the difference between the ditch water level and the land surface elevation is over two metres at this point. Around $x = 200$m the upconing because of the small drainage ditch mentioned in Figure 10 is visible.

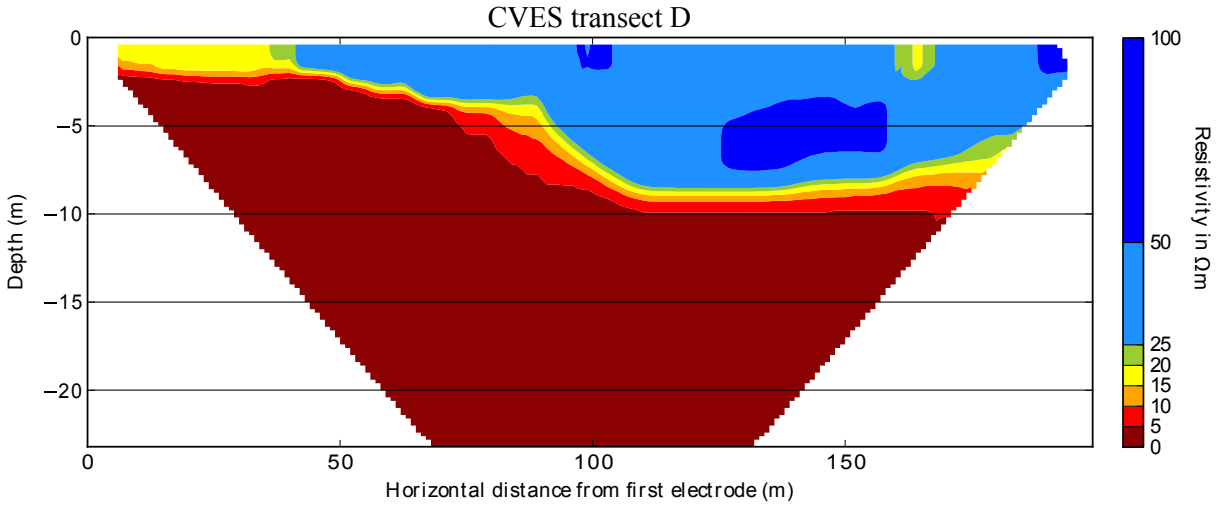

Figure 12: Transect D shows the abrupt beginning of the sandy creek ridge in the middle of the figure. To the left the soil is rich in clay, and there are layers of peat in the subsurface, according to the farmer who had to build his house here on deep foundations.

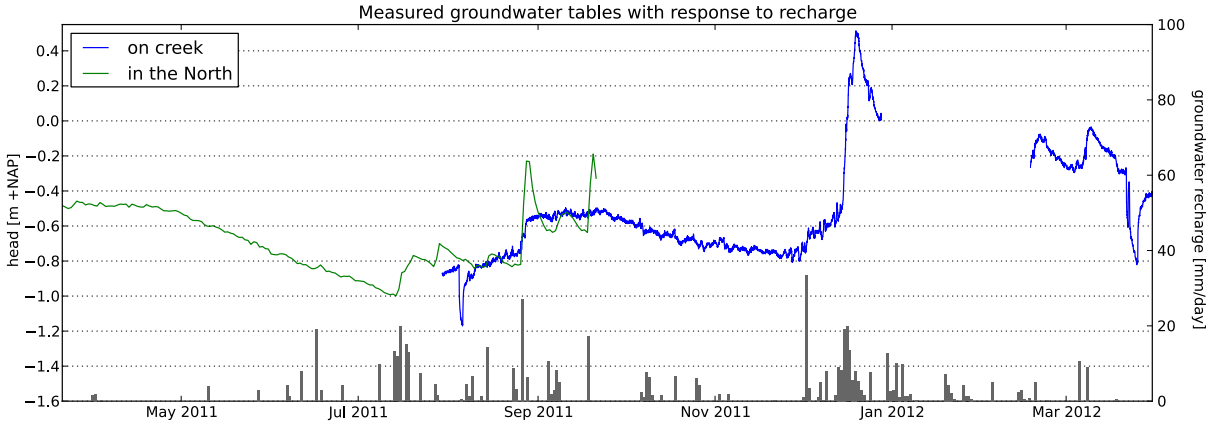

Figure 13: Measured groundwater table fluctuations at the locations 800 m apart. A simplistic calculation of groundwater recharge, as precipitation minus reference crop evaporation, is also plotted. This daily data comes from the Royal Dutch Meteorological Institute (KNMI), weather station Vlissingen, approximately 10 km from the site.

6 Model setup

The model was created to be able to answer the research questions of this work. MOCDENS3D [*Oude Essink*, 1999] was chosen as a numerical code because both Deltares supervisors had experience working with this code, and the author of the code was also present for advice. The USGS counterpart SEAWAT, based on MODFLOW and MT3DMS, was also an option but for models of this size experiences from our supervisors were better with MOCDENS3D. MOCDENS3D consists of an adaptation of MODFLOW for density dependent groundwater flow, combined with MOC3D [*Konikow et al.*, 1996]. The groundwater flow equation with an added buoyancy term is solved by adapted MODFLOW-96 code. The advection-dispersion equation is time-splitted, calculated first advection only using the method of characteristics, followed by finite difference methods to calculate dispersion.

The numerical model operates on a discretised domain, with grid cells in which all variables and parameters are uniform. To keep the computational time within an acceptable range, the domain is divided into 2×10^6 grid cells. A 10 m horizontal grid spacing was deemed sufficiently small to accurately model flow in the approximately 300 m wide creek bed. A vertical resolution of 0.5 m was chosen to be able to accurately model the freshwater lens depth. An overview of the model properties and parameters is presented in Table 2.

The hydraulic conductivity model input consists of the mean of fifty realisations of a combination of the REGIS II and GeoTOP models. REGIS II is a national hydrogeological model that maps the locations of the different hydrogeological units in the subsurface, discretised into 100×100 m^2 grid cells [*Vernes and van Doorn*, 2005]. GeoTOP has the same resolution but is a more detailed model that maps the top thirty metres of the subsurface [*Stafleu et al.*, 2011]. The geology provided by GeoTOP is conceptually illustrated in Figure 14. Whilst the cross-section path lies south of the model domain, tidal channel deposits are also present, coloured light green in the figure.

Table 2: Model properties and parameters used in the reference scenario.

model area	$2.56\,\mathrm{km}^2$
horizontal cell size	10 m
vertical cell size	0.5 m until −25 m +NAP, then gradually coarser
bottom of model domain	−87 m +NAP
number of cells	$160 \times 160 \times 80$
number of active cells	2 000 358
number of particles per cell	27
stress period length	6 months
winter recharge rate	1.4 mm/day
summer recharge rate	−0.2 mm/day
timestep groundwater flow	1 month
timestep salt transport	1–3 days, automatically determined
porosity	0.35
anisotropy k_h/k_v	1.4
longitudinal dispersivity α_L	0.1 m
transverse dispersivity α_T	0.01 m
effective diffusivity D_e	$8.64 \times 10^{-5}\,\mathrm{m}^2/\mathrm{s}$
specific yield S_y	0.15, assigned to upper active cells only
confined storage coefficient S_s	$1 \times 10^{-5}\,\mathrm{m}^{-1}$, assigned to all other cells
head closure criterion	1×10^{-6} m

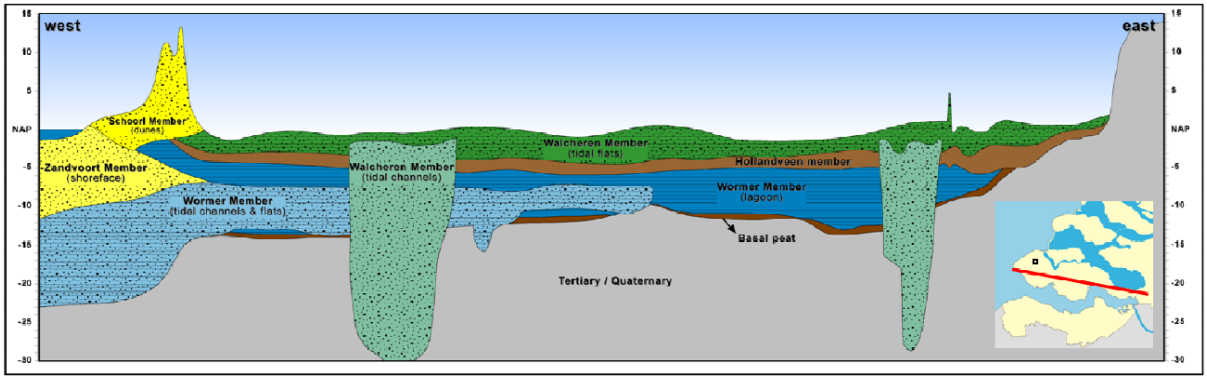

Figure 14: Schematic cross-section of the Holocene deposits represented in GeoTOP. Inlay shows path of the 70 km long cross-section in red, and the approximate model domain in black. After Stafleu et al. [2011].

6.1 Boundary conditions

On the bottom of the model domain MODFLOW's implicit no-flow boundary conditions are retained. The top of the model is the same as the highest point of the creek ridge, at 1.5 m +NAP. The cells that lie above the ground surface are the only cells that have been deactivated. The bottom boundary lies at −87 m +NAP. According to the REGIS II national hydrogeological model there is an aquitard present at this height, with a k_v value of 2.5×10^{-4} m/day. Therefore it is a reasonable approximation to have a no-flow boundary at this depth.

For the boundary conditions on the sides there are no natural or known hydraulic boundaries in the vicinity of the area of interest, the creek ridge. There are calibrated summer and winter heads available from the regional MOCDENS3D groundwater model [*van Baaren et al.*, 2012], with grid cells of 100 m wide. These heads are used on the boundary conditions, together with a specified conductance implemented in the *General-Head Boundary Package*. With this package neither the head nor the flux is prescribed in the boundary cells, but there is a flow that is proportional to the difference between the calculated head in the boundary cell and the corresponding prescribed head from the regional model, $Q = C\Delta H$. The proportionality constant $C = k_h A/L$ is the conductance between the boundary cell and the fictional constant head reservoir. A value for C of $1\,\mathrm{m}^2$/day was used on all sides of the model, as this gave satisfactory results. To minimize the effect of errors introduced by the boundary conditions, the model boundaries have been placed at a distance of around 500 m from the edge of the area of interest.

When water flows from the general-head boundary into the model, it has been set to have a chloride concentration of 18 630 $mg\ Cl^-/l$, equal to seawater. Above the fresh-salt interface this will be incorrect and introduce extra salt to the system since there is regional flow from north to south, with a difference in head of on average 0.4 m between the north and south side (1600 m apart).

6.2 Initial conditions

The objective for the reference scenario was to recreate the current chloride distribution as it was measured in the field. The assumption made was that the current chloride distribution is more or less in equilibrium. By starting off the model with a completely salt domain (18 630 $mg\ Cl^-/l$), and letting it rain for 150 years until the freshwater lenses reach an equilibrium, the current chloride distribution is approximately recreated. Influence of any historical variations is not included in the model because of difficulties modelling this and contributing little to the results.

The initial head distribution for the transient model is the steady-state head distribution, which was calculated separately.

6.3 Minimizing model error

Initially model runs were done on standard desktop computers. In calibrating the model, many times it had to be run, adjusted and rerun. For this part it was important that model run times were limited such that steady progress was possible. Rough head calibration was done first, since this hardly takes run time. Then long runs were done, to let the lens grow to equilibrium. Both final groundwater table (different now there is a lens

beneath), and concentration fields then had to be calibrated to the available observations. The model runs presented in this work had run times of up to two weeks, longer than the calibration runs, because parameters were set for accuracy, not speed.

Before settling on the final model setup choices, several tests where done to aid in taking these decisions, keeping the model error to an acceptable level. These tests are also presented here, both as a justification for this model setup and because they may be of interest to other groundwater modellers.

6.3.1 Transient or steady state

If MODFLOW is set to transient flow, it calculates heads as they, with time, adapt to the stresses put into the model. Stress periods can be divided into flow time steps. After every flow time steps the heads are recalculated, such that the solution is an accurate adaptation with time to the stresses provided. If MODFLOW is set to calculate steady state heads, the time derivative of head is set to zero in the groundwater flow equation. The model will calculate a solution that is in equilibrium, effectively what would be the head distribution after heads have fully adapted to model stresses. Calculating a transient model takes considerably longer than a steady state model. Therefore, if, the error of the steady state assumption is not too large, modellers prefer to calculate with steady state flow.

Whether steady state is acceptable depends especially on hydraulic conductivity, the magnitude of the differences between the stress periods (recharge rates etc.) and the length of the stress periods. Groundwater flow normally does not reach equilibrium within days or even months. For yearly stress periods the model may adapt quickly enough, which, combined with small differences between stress periods, can make steady state modelling acceptable. The model in this work is designed for half-yearly stress periods, making it worth researching the magnitude of the steady state error for this model.

Two models, with as only difference steady state versus transient, were run until the fresh-salt system was in equilibrium. Then the resulting heads from the last year were taken, and plotted at two different locations; in the sandy creek and in the reclaimed marshland, both at the top of the model (Figure 15). Several things are worth noting. The transient heads adapt more quickly in the permeable creek, resulting in a smaller difference between transient and steady state summer heads at this location. This is most likely due to the difference in hydraulic conductivity of the soil; one can drain a sandy soil much faster than a clay soil. On both locations heads rise faster than they lower, and heads rise equally fast at the start of winter. This is expected to be because whilst drainage often involves long horizontal travel distances, recharge is (in the model) directly added to the groundwater table. Therefore for the transient case there are not only more moderate heads during most months (making for a 2× thinner interface on the creek), but the yearly average head is also higher. On the creek this difference is 4 cm, which in this case translated to a deepening of the interface of 2 m. This already unacceptable difference will only be worse outside of the sandy creek. Thus the decision was made to accept the extra runtime and compute only transient flow.

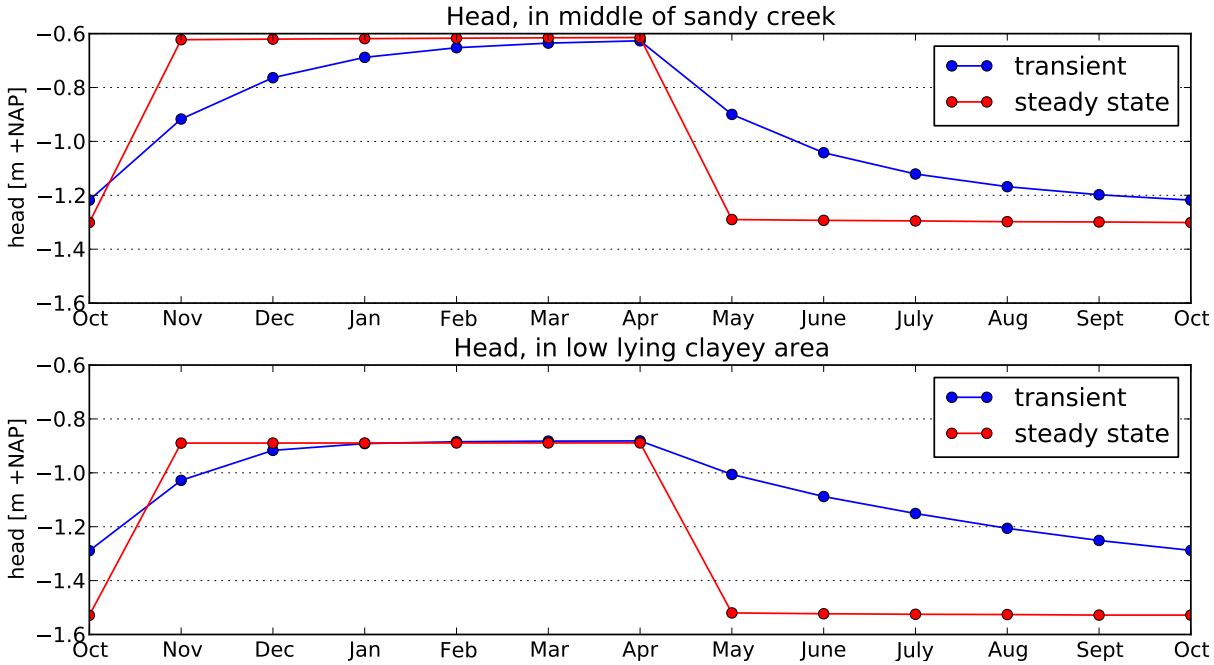

Figure 15: Typical difference in heads of a transient model compared to a steady state model.

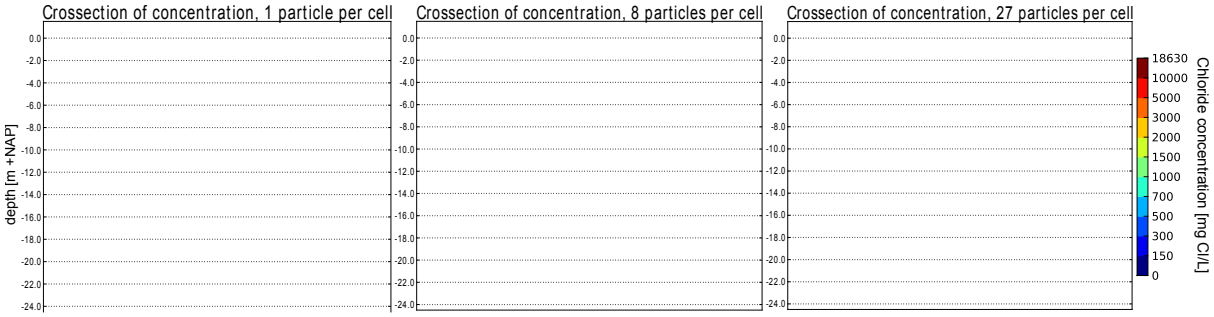

Figure 16: Equilibrium concentrations achieved using 1, 8 and 27 particles per cell for the particle tracking procedure used in calculating the solute transport. Shown is one model row (row 90), which is 1600 m wide.

6.3.2 Number of particles per cell

The code that handles the advective solute transport in MOCDENS3D is MOC. Internally MOC puts a certain number of particles in a cell, and allows the particles to advect with the computed flow, possibly into neighbouring cells. At the end of a solute transport step the cells are assigned concentrations according to the concentrations of the particles. More particles thus means more accurate results. The number of particles that MOC puts into a cell can be set by the user. This significantly affects model runtime, so different amounts are compared to make a good decision, see Figure 16. One particle is clearly not acceptable, but the difference between 8 and 27 particles is already rather small. The choice was made to use 27 particles, because it should be more accurate. However for non-final model runs 8 particles were used allowing for more rapid model development.

6.4 Arriving at current situation

The model was started with a completely salt domain. This model was simulated until the freshwater lens on the creek ridge approximately reached an equilibrium and no longer grew. This growth of the freshwater lens in the middle of the ridge is plotted in Figure 17. After 150 years the interface lies 15 m below ground level (BGL), with a 5 m thick mixing zone (between 150 and 10000$mg\ Cl^-/l$). The model results at the end of this run are supposed to model the fresh-salt distribution as it is currently observed in the field. Hence these results are referred to as the 'current situation'.

The three dimensional concentration field was combined with a surface elevation map to calculate a 2-D map with the interface depth in metres below ground level (Figure 18). After that the heads are plotted in the first model layer where all cells are active, at -1.25 m +NAP (Figure 19). Half-year stress period models do not compare to the hourly heads that the divers provide. The model was adapted to use daily stress periods and actual recharge, such that it could be validated against the head measurements (Figure 20).

CVES transects A and B were used in model calibration. For instance the hydraulic conductivity of parts of the sandy creek, as given by the GeoTOP model, were deemed to low. The creek bed consists of fine well sorted sand. The conductivity was calculated based on median grain size and porosity using the Kozeny-Carmen equation,

$$K = \left(\frac{\rho_w g}{\mu}\right)\left(\frac{n^3}{(1-n)^2}\right)\left(\frac{(d_{50})^2}{180}\right)$$

where ρ_w/μ is the unit weight/viscosity of water, n is porosity, and d_{50} is median grain size (modified from Bear, 1972 by [*Fitts*, 2002]). This resulted in a higher conductivity of 2.6 m/day, which was then used in the model. A concentration profile of transect A can be seen in Figure 21. CVES transects C and D are only for validation. Figure 22 shows the model result along transect C.

7 Effect of measures on model

Two different measures to increase the freshwater lens are tested with the model. These are both implemented as scenarios that start from the current situation and run until a new equilibrium is reached. This takes 50 years, and the results given are thus after 50 years of running the scenario. This is a long time for a return on investment, however note that the lens depth over time resembles an exponential decay curve, with half of the total change accomplished after 10 years. Changing climate conditions and rising sea levels are not taken into account, even though these will very likely put extra pressure on the coastal groundwater system in Zeeland [*Goes et al.*, 2009]. However the presented measures to increase the freshwater lens can just as easily be viewed as ideas for climate change adaptation.

7.1 Raised ditch water level

As can be seen in both measurements (Figure 11) and model results (Figure 19), much of the freshwater of the sandy creek is lost to the section of the brackish primary ditch that

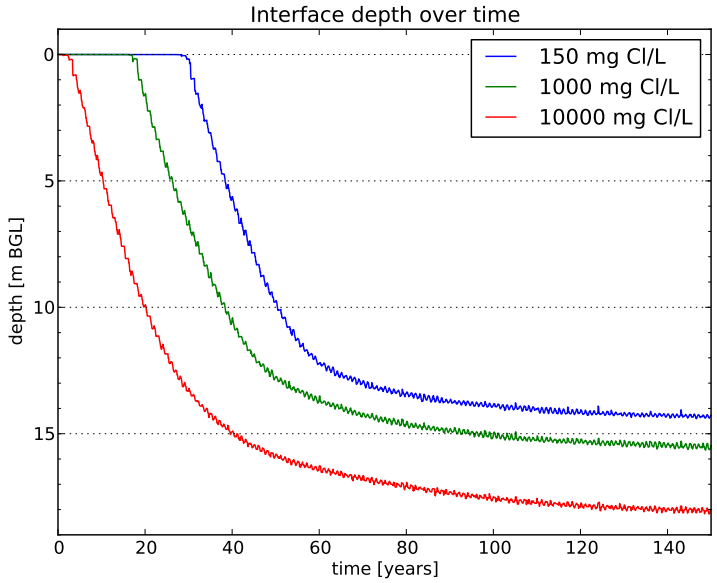

Figure 17: Plot of the depth of three different concentrations over time in the middle of the sandy creek. Initially the whole domain is saline, but after 150 years the freshwater lens approximately reaches equilibrium.

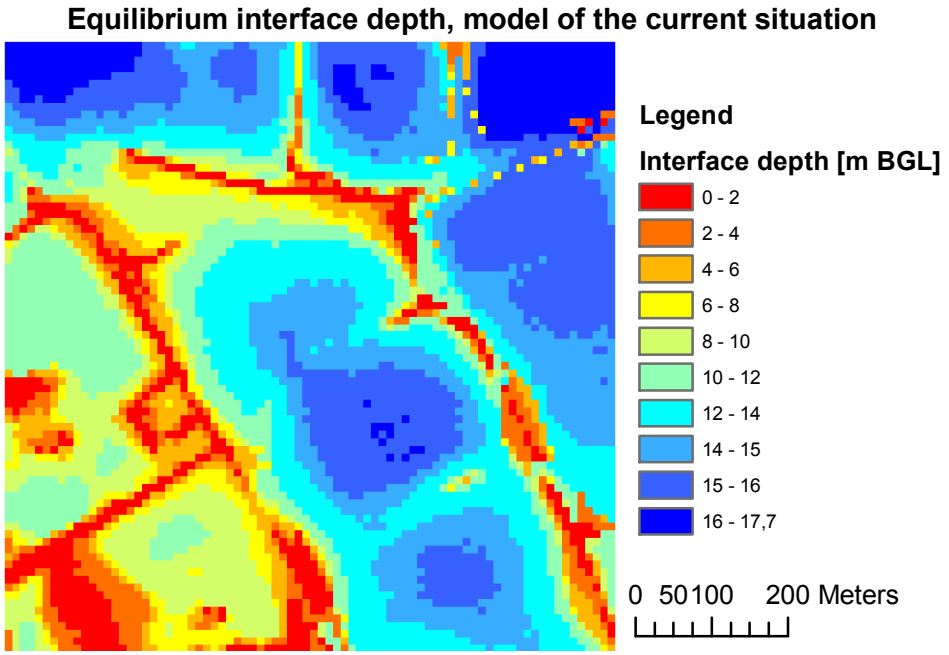

Figure 18: The depth to the fresh-salt interface in the area of interest. On the creek ridge the lens is approximately 15 m thick. The brackish primary ditch, which has a water level of -1.2 m +NAP, hinders the development of a larger freshwater lens. To the right of the sandy creek this effect is reduced by a less permeable soil between the sandy creek and the primary ditch. But in the top of the figure, where the primary ditch cuts through the sandy creek, freshwater lens development is hindered severely as rainwater easily flows through the sand into the primary ditch two metres below the ground level of the ridge.

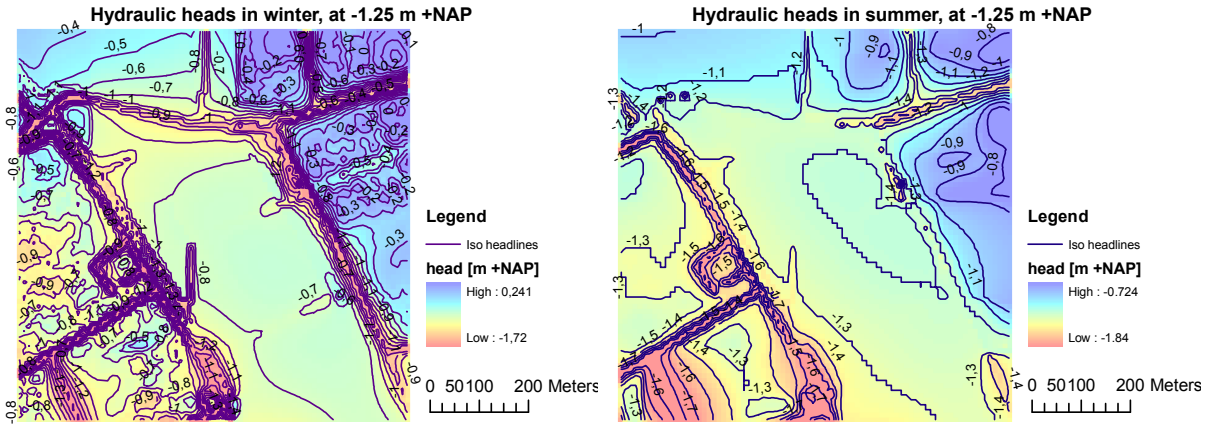

Figure 19: Left: groundwater levels at the end of the winter stress period. Recharge causes the table to bulge over plots of land, especially so in less permeable regions. Right: In summer there is a 0.2 mm/day net evaporation, flattening the bulges of the groundwater table.

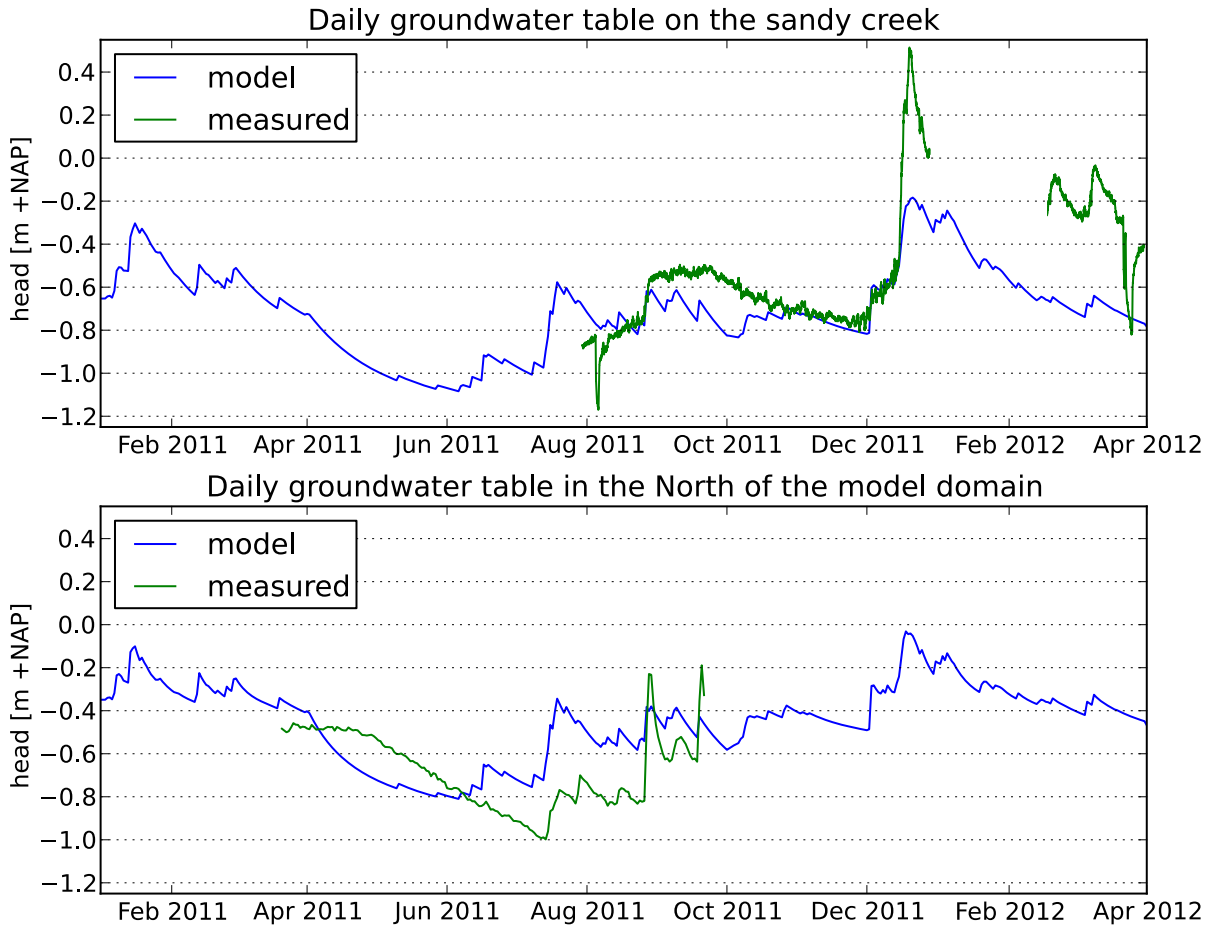

Figure 20: Comparison of the model using daily stress periods and actual recharge, to the continuous head measurements in the piezometers. Whilst the model is not designed for this purpose, it is assuring to see the model comparing favourably to the measured data, especially on the sandy creek. The measured response to the December 2011 heavy rains is more intense than modelled. This may be caused by unsaturated zone effects, which the model does not support.

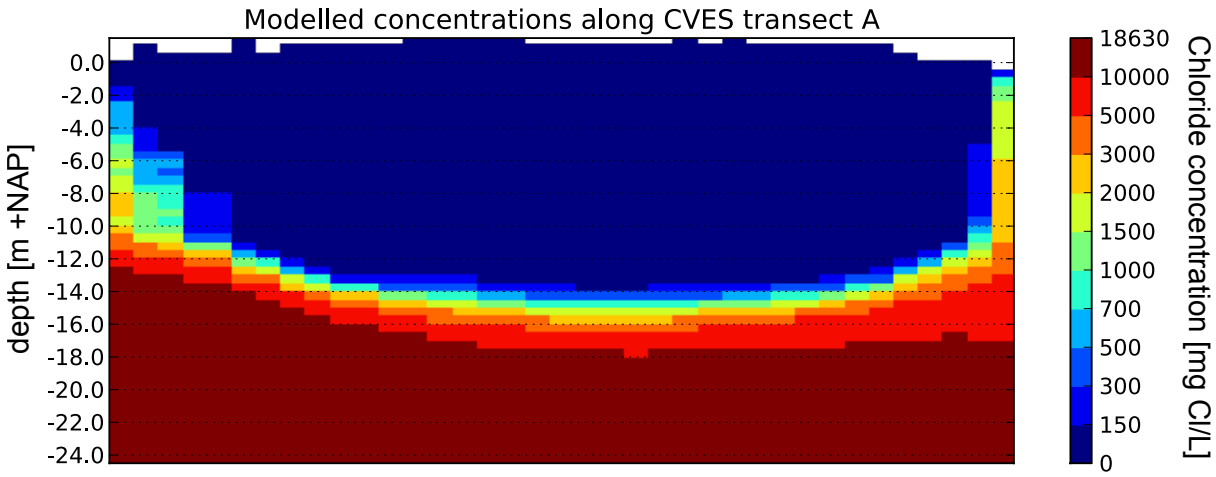

Figure 21: This concentration profile is similar to CVES transect A, shown in Figure 9 on page 13. Maximum lens thickness is accurate within 1 m. The measured electrical resistivity is lower near the edges of the transect, suggesting a less wide freshwater lens; a modelling error. However it is possible that the lens is wider than suggested in the CVES image, because towards the transect edges the soil becomes rich in clay, which also causes lower resistivity values. It should be noted that CVES transect A was used to calibrate the model.

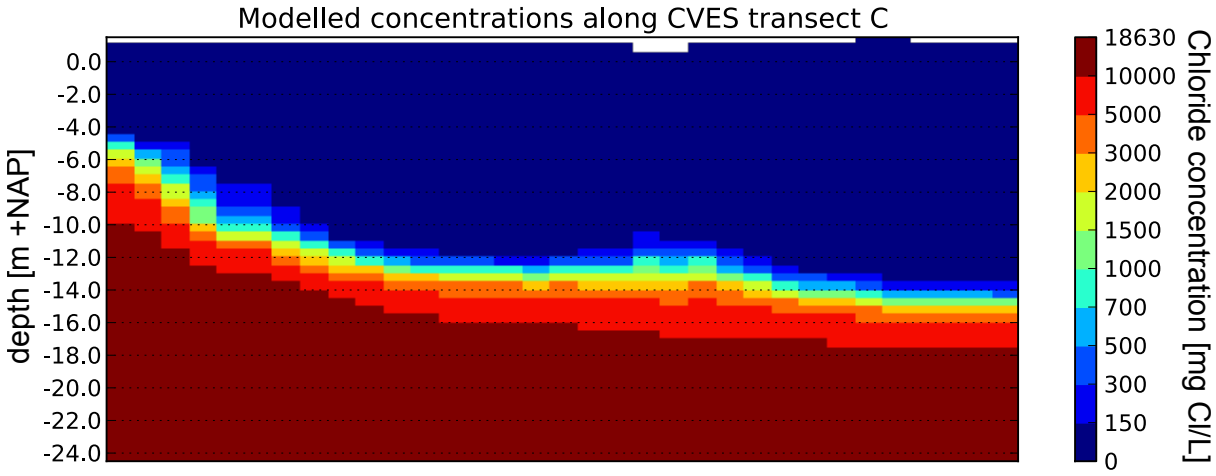

Figure 22: This concentration profile is similar to CVES transect C, shown in Figure 11 on page 14. CVES transect C was made after the model development stopped, and is thus used as a validation of the model. There is close agreement between measured and modelled result, the slowly thinning lens towards the left and small upconing towards the small drainage ditch can be seen in both figures. Also since the entire transect lies on the sandy creek, there will be no significant influence of the subsurface material on the CVES profile.

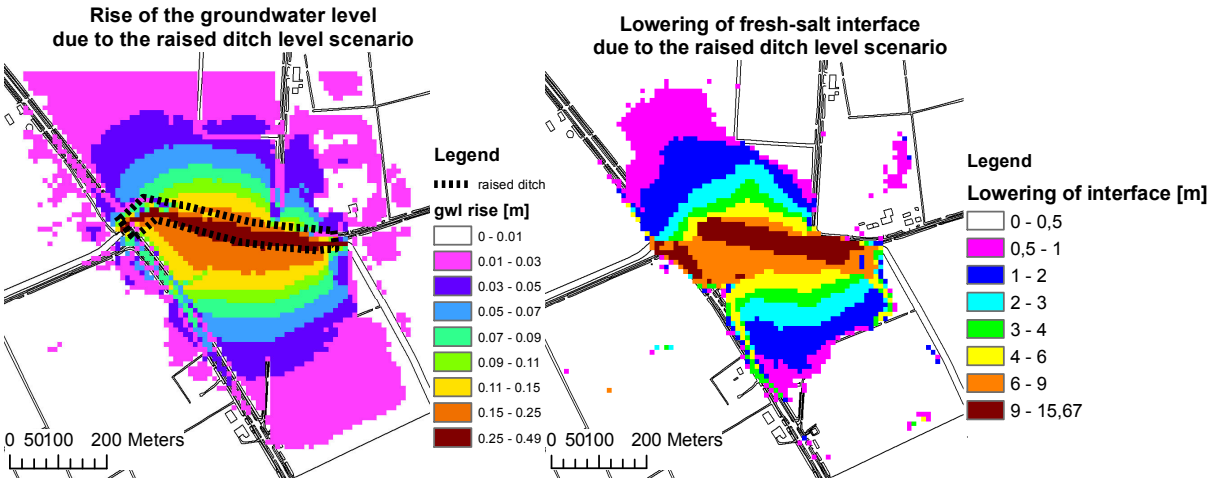

Figure 23: The effect of raising the water level of a part of the primary ditch (dotted) by 0.5 m on winter heads (left) and interface depth (right).

cuts deep through the sandy creek bed. From this an interesting question was raised: what would happen if this section of the primary ditch was somehow dammed off, such that the surface water would become fresh and the water level would rise by 0.5 m, to −0.7 m +NAP? This work will not go into the matters concerned with implementing this in the field, but merely shows what would happen if such a thing were to be done (see Figure 23). Since the water level increases by 0.5 m, the groundwater table will rise by the same amount in the immediate vicinity. However the figure shows that even 200 m from the ditch the table would rise by 6 cm because of this measure. The presented water table rise is not expected to trouble any farmers, since it mainly rises on the sandy creek ridge, where the groundwater table is deep enough. Before there was no lens at the primary ditch, now the interface is at 15 m depth, which happens to be the same as the maximum lens thickness lower on the sandy creek. Effectively the upconing towards the primary ditch no longer exists, and the lens now becomes around 15 m thick along the entire ridge pictured.

7.2 Artificial recharge through a controlled drainage system

Fresh groundwater from the creek ridge is not only lost by flowing directly into the ridge-cutting primary ditch. It also flows out through the small drainage ditch on the ridge, and the pipe drains that are placed approximately one metre below the surface across the sandy creek. Two of these pipe drains lie a metre deeper than the rest, these drain the sandy creek especially intensely. Drainage on the sandy creek is necessary to drain excess rainwater away, but as it is currently it is also keeping the groundwater table down in periods when it is allowed to be close to the surface. This also prevents the formation of a thicker freshwater lens.

A controlled drainage system is another drainage system, that would replace both drainage ditch and current pipe drains. In the particular controlled drainage system considered here, the pipe drains are placed closer together and deeper, such that they are always below the groundwater table. Rather than discharging directly to surface water, they are connected to a larger collector drain. At the end of this collector drain

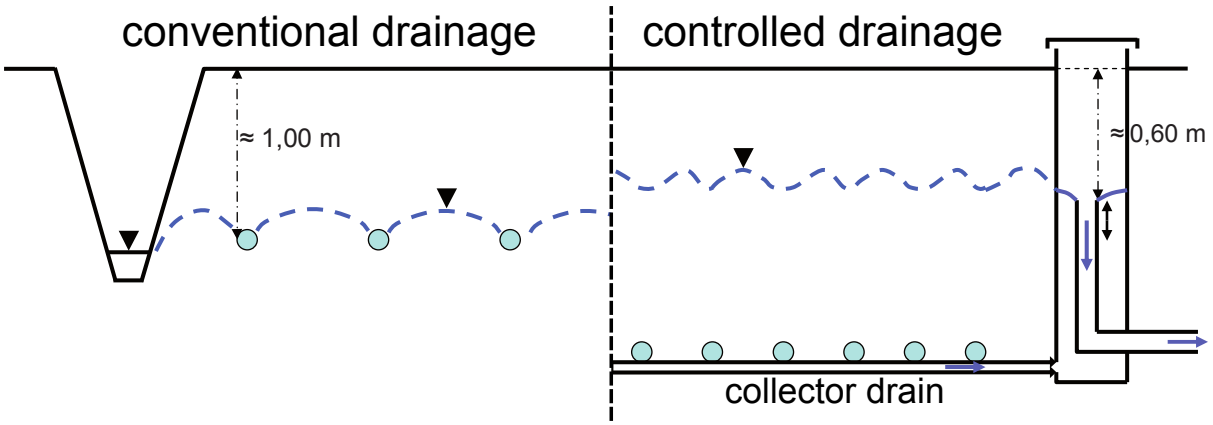

Figure 24: Illustration showing the difference between conventional and controlled drainage. On the right side the drainage level is controlled by setting the height of the outflow tube, the so-called 'van Iersel' system. The outflow tube can discharge into a primary ditch. Infiltration is also possible with the controlled drainage system, one only needs to pump water into the outlet instead. Image after van Bakel et al. [2008].

the drainage level can be controlled manually. When the table rises above the drainage level, it will be discharged from the collector drain to the surface water. This allows for greater flexibility in controlling the water table. Furthermore, since drainage happens at a deeper level, less nutrients are washed out [*van Bakel et al.*, 2008]. The difference is illustrated in Figure 24.

The idea was to make a scenario of artificial recharge through a controlled drainage system that would be realistic, such that it can later can be installed and tested in the field. However logistics, such as where the to be infiltrated water comes from, are not considered. Also water quality issues are not part of this work, but will be the focus of continuing research under the Knowledge for Climate programme. In the model the natural recharge rate is set to 1.4 mm/day during the winter half year stress periods and -0.2 mm/day during the summer half year stress periods. An artificial infiltration area was defined on the sandy creek. In this area 1 mm/day of extra water was injected at a depth of two metre below the surface. This was only done during the winter months of November, December, January and February, when there is generally a rainwater surplus. To make this possible the model was changed to use monthly stress periods instead.

The final result of this scenario is shown in Figure 25. As a part of this scenario the small drainage ditch and the two metre deep drainage pipes are removed. Therefore the head increase is the largest at these locations. Because these two features are removed, the infiltrated water does not end up in the primary ditch as fast, making it more effective. However in the north of the infiltration area the infiltrated water easily flows into the primary ditch cutting through the sand, making infiltration here less effective. The farmers cautioned that the groundwater table is not allowed to rise more than a few centimetres directly to the east of the infiltration area. The surface elevation here is considerably lower than on top of the ridge, and the soil is rich in clay. At some locations the soil is already too wet for good crop production. The infiltration area is limited to the sandy soil, and the groundwater table does not rise more than is allowed by the farmers. Since the upconing towards the drainage ditch and deep drainage pipes disappears, the lowering of the fresh-salt interface is much larger around these areas. The thickening of

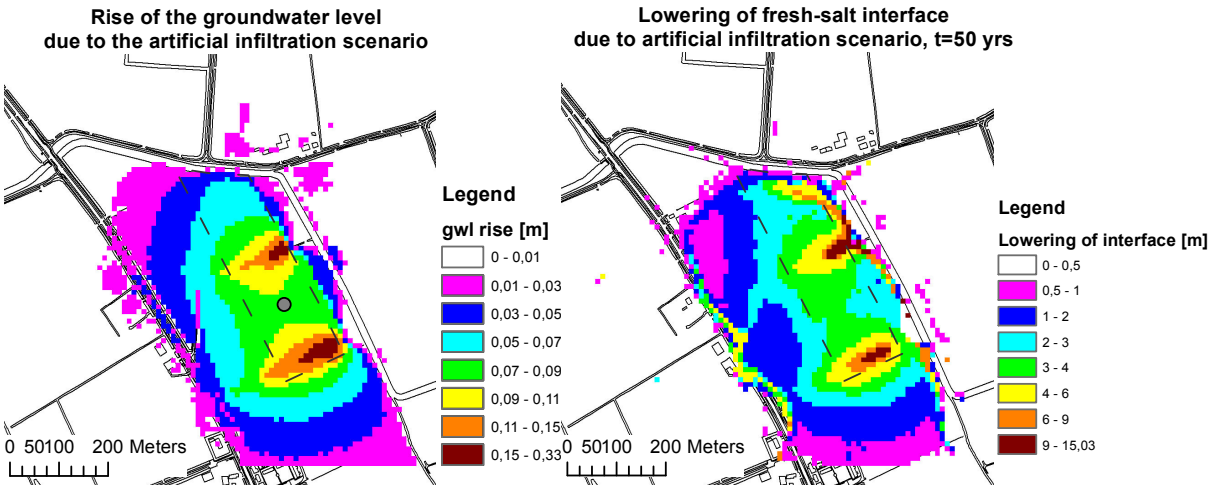

Figure 25: Left: the effect of the artificial infiltration scenario on heads, one month after infiltration stopped. Artificial infiltration takes place inside the area outlined with the dotted line. The grey dot marks a virtual observation well. Right: the freshwater lens thickens by minimally 2 m inside the infiltration zone.

the lens spreads around the sandy creek outside of the infiltration area, away from the primary ditch.

Figure 25 shows the increased lens thickness after fifty years of winter infiltration, when it is close to equilibrium again. The growth of the freshwater lens after ten years is shown in Figure 26. As stated earlier, this amounts to approximately half of the equilibrium growth.

A more detailed figure of the temporal head variations with and without artificial infiltration is shown in Figure 27. During the four infiltration months in winter, the head rises faster than normal, growing to a 12 cm difference. When the infiltration is stopped, this falls back to 8 cm in a month, reducing further over summer.

8 Discussion

After this work, a controlled drainage system will be installed into the sandy creek. Pilots with artificial infiltration through this system will also be performed. This will be a true validation for the model results. But judging by the overall performance of the model it is likely not too far from the truth.

That said, there are several limitations to this research. Whilst MOCDENS3D is accurate for simulating freshwater lens development, it was also used to study the effect of drainage. If the model would be solely for this purpose, a smaller, perhaps two dimensional model with unsaturated flow would serve better. Even without artificially infiltrating, the controlled drainage system will very likely be beneficial for growth of the freshwater lens. But this was not modelled, partly because this depends heavily on how the system is controlled by the farmer. Nevertheless modelling the hydrogeological system in the whole area gave good insights into the importance of smart drain and ditch placement.

Since the regional model by van Baaren et al. [2012] was used to provide steady

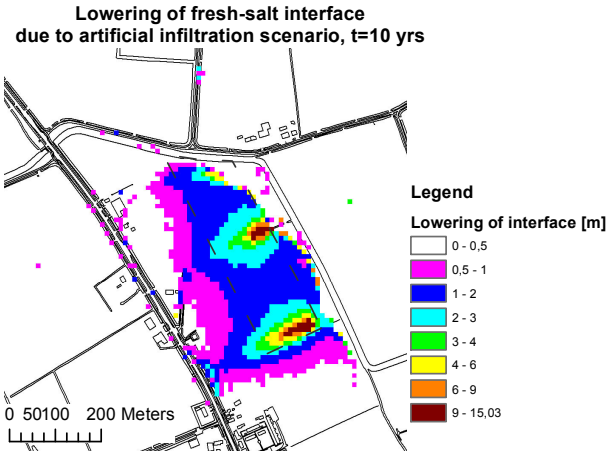

Figure 26: Thickening of the freshwater lens due artificial infiltration, ten years after winter infiltration started.

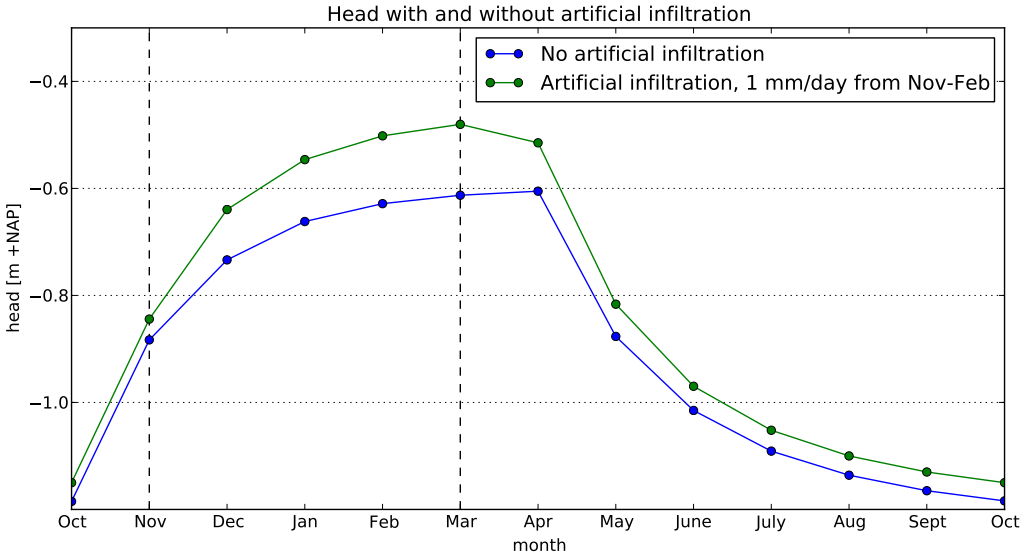

Figure 27: Monthly head comparison between artificial infiltration and the reference scenario, at the location of the grey marker in Figure 25. Injection only takes place from November 1 until March 1.

state winter and summer heads on the boundary conditions, the accuracy of the regional flow relies on the accuracy of the regional model, which has 10× bigger grid cells. The concentrations on the boundaries were set to seawater concentrations. This was initially done to keep things simple and conservative, however since heads and concentrations are linked this introduced incorrect flow patterns around the model boundaries.

The hydraulic conductivity grids also came at a 10× coarser resolution. Horizontally these maps were interpolated to reduce unrealistic flow patterns. They were also slightly tweaked based on field data, something which the authors of GeoTOP say is neccessary to make accurate local groundwater models with the data [*Stafleu et al.*, 2011]. The hydraulic conductivity data introduced one of the largest uncertainties into the model, which is common for 3-D groundwater models.

To recreate the current situation an initially saline model was run until an equilibrium was reached. This assumes that the current situation is in equilibrium. To what degree this is true is hard to determine, since almost all measurements were done this year, and little is available from the past that can give information over the current movement of the freshwater lens. In the north-west corner of the model area is a deep piezometer with chloride concentration time series between 1984 and 1996 (accessible through DINOLoket), but these are at 25 and 50 metres deep, below the freshwater lens at this location. Still, these groundwater sample measurements show relatively stable concentrations of around $16000 mg\ Cl^-/l$ and $19000 mg\ Cl^-/l$, respectively for 25 and 50 metres deep.

Fieldwork and model development was focused on, and calibrated for, the creek ridge. However the surrounding land is also included in the model. The model results here can become less accurate due to closer proximity to the model boundary. However, looking at Figure 18, it still came as a surprise how thick some of the freshwater lenses were in the surrounding lands. To the east of the creek ridge of interest, modelled freshwater lenses were approximately equal to the calibrated freshwater lens in the center. Looking at both the soil map (Figure 2) and elevation map (Figure 3), it is an area above NAP with also sandy creek bed soils. This makes the model results more plausible, but since there are no measurements there it is unconfirmed. To the left of the sandy creek, elevations are around NAP, and soils are heavier. One short path with the EM31 over this terrain revealed high salinities (Figure 6), in line with the experiences of the farmers. Thin rainwater lenses, less than 5 m are thus expected. At the location of said EM31 readings the model predicts 5 m thick lenses. However what is more surprising is that on larger plots of low lying heavy soils, the model predicts lenses up to 10 m. Although there are no measurements here this is considered unlikely. The model might underpredict seepage flux, and because of low permeabilities large groundwater table bulges develop over the bigger plots in winter, pushing down the salt.

9 Conclusion

The fossil sandy creek ridge north of Serooskerke, Walcheren lies on average one metre above NAP, but is neighboured by reclaimed salt marshes that are up to 40 centimetres below NAP. To investigate the occurrence of a freshwater lens beneath the surface of the creek ridge, a range of geophysical measurements were done. After getting a good

image of the outline of the freshwater lens with the EM31 measurements, the CVES measurements were able to accurately show the depth of the freshwater lens (up to 14 m on the ridge), but also where upconing occurred, for instance to a deeply placed drainage pipe.

Hydrogeologically, the sandy creek lies in a low-lying saline seepage area, where most of the ditches attract saline seepage from below. This mixes with rainwater flowing into the ditches from the sides. For the growth of freshwater lenses, pressure from the freshwater is essential to push back the slowly upwards seeping salt. Therefore it is not good for the freshwater lens if rainwater is quickly drained towards the ditch, as this will bring down the groundwater table in the ridge to near the water level in the ditch. One particularly wide and deep ditch runs east of the creek ridge, and cuts through the sandy creek in the north of the model domain. To the east, the freshwater lost to the primary ditch is limited by a strip of low permeability soil 'protecting' the sandy creek from the influence of the ditch. However to the north there is no such strip and both modelled heads (Figure 19) and measured lens thickness (Figure 11) show a large influence of this section of the primary ditch.

Modelling results showed that replacing the current conventional pipe drainage with controlled drainage on the sandy creek prevents unnecessary drainage, making it possible to retain higher groundwater tables, which over time translates to a thicker freshwater lens. The freshwater lens can also be seen as a reservoir from which water can be pumped for irrigation during dry spells in summer. To try to keep this practise sustainable and prevent upconing into the horizontal well, extra water can be infiltrated through the controlled drainage system when there is excess water available. In the model this method is successful in pushing down the fresh-salt interface, but for application in the field close monitoring of the dynamics of the lens is still advised, in order to get a good idea what yearly pumping volumes are sustainable.

Besides injection of freshwater, the effect of a surface water level rise of 50 cm in the section of the primary ditch that goes over the creek ridge was investigated. The model predicts that this rise of 50 cm greatly reduces freshwater outflow to this ditch, basically resulting in a continuous freshwater lens crossing over the (now fresh) ditch section.

References

de Louw, P. G. B., S. Eeman, B. Siemon, B. R. Voortman, J. Gunnink, E. S. van Baaren, and G. H. P. Oude Essink (2011), Shallow rainwater lenses in deltaic areas with saline seepage, *Hydrol. Earth Syst. Sci. Discuss.*, *8*(4), 7657–7707, doi: 10.5194/hessd-8-7657-2011.

Fitts, C. R. (2002), *Groundwater Science*, 450 pp., Academic Press.

Goes, B. J. M., G. H. P. O. Essink, R. W. Vernes, and F. Sergi (2009), Estimating the depth of fresh and brackish groundwater in a predominantly saline region using geophysical and hydrological methods, Zeeland, the Netherlands, *Near Surface Geophysics*, *7*(5-6), 401–412, doi:10.3997/1873-0604.2009048.

Konikow, L., D. Goode, and G. Hornberger (1996), A three-dimensional method-of-characteristics solute-transport model (MOC3D), *U.S. Geological Survey Water-Resources Investigations Report 96-4267*, p. 87.

Oude Essink, G. H. P. (1999), Simulating 3D density dependent groundwater flow: the adapted MOC3D, *Proc. 15th Salt Water Intrusion Meeting, Ghent, Belgium*, pp. 69–79.

Oude Essink, G. H. P. (2001), Salt water intrusion in a three-dimensional groundwater system in the Netherlands: A numerical study, *Transport in Porous Media*, *43*, 137–158, 10.1023/A:1010625913251.

Panday, S., P. S. Huyakorn, J. B. Robertson, and B. McGurk (1993), A density-dependent flow and transport analysis of the effects of groundwater development in a freshwater lens of limited areal extent: The Geneva area (Florida, U.S.A.) case study, *Journal of Contaminant Hydrology*, *12*(4), 329 – 354, doi:10.1016/0169-7722(93)90004-C.

Pauw, P. (2011), Overview of common field measurements applicable in the research on freshwater lenses in coastal areas, Knowledge for Climate, Deltares, Wageningen UR.

Post, V., H. Kooi, and C. Simmons (2007), Using hydraulic head measurements in variable-density ground water flow analyses, *Ground Water*, *45*(6), 664–671, doi: 10.1111/j.1745-6584.2007.00339.x.

Pyne, R. D. G. (2005), *Aquifer Storage Recovery: A Guide to Groundwater Recharge Through Wells*, 2nd ed., 620 pp., ASR Press.

Sanford, W., and J. Pope (2010), Current challenges using models to forecast seawater intrusion: lessons from the Eastern Shore of Virginia, USA, *Hydrogeology Journal*, *18*, 73–93, doi:10.1007/s10040-009-0513-4.

Stafleu, J., D. Maljers, J. L. Gunnink, A. Menkovic, and F. S. Busschers (2011), 3D modelling of the shallow subsurface of Zeeland, the Netherlands, *Netherlands Journal of Geosciences*, *90*(4), 293–310.

Stuyfzand, P. J. (1986), A new hydrochemical classification of watertypes: principles and application to the coastal dunes aquifer system of the Netherlands, *Proc. 9th Salt Water Intrusion Meeting, Delft, the Netherlands*, pp. 641–655.

Stuyfzand, P. J. (2010), Water technology as a tool box for self-sufficient regional water supply, *proposal extract*, Knowledge for Climate.

Stuyfzand, P. J., and A. Doomen (2004), The Dutch experience with managed aquifer recharge and storage: a review of facilities, techniques and tools, *Kiwa N.V. / NWP*, *5*(1).

van Baaren, E. S., G. H. P. Oude Essink, G. M. C. M. Janssen, P. G. B. de Louw, R. Heerdink, and B. Goes (2012), Verzoeting/verzilting freatisch grondwater in de provincie Zeeland, rapportage 3D dichtheidsafhankelijk grondwatermodel, Concept Deltares.

van Bakel, P. J. T., E. M. P. M. van Boekel, and G. J. Noij (2008), Modelonderzoek naar effecten van conventionele en samengestelde, peilgestuurde drainage op de hydrologie en nutriëntenbelasting, *report*, Alterra, Wageningen.

van Betuw, T. W. J. (1952), De bodemkartering van Nederland, deel XII: De bodemkartering van Walcheren. Verslagen landbouwkundige onderzoekingen nr.: 58.4, Stichting voor Bodemkartering.

van der Straat, A. (1986), Kreekruggen, *report*, Provinciale Waterstaat Zeeland, Middelburg, Zeeland.

van Meerten, J. J. (1986), Kunstmatige infiltratie in kreekruggen, M.S. thesis, Delft University of Technology, Delft.

Vernes, R. W., and T. H. M. van Doorn (2005), Van gidslaag naar hydrogeologische eenheid toelichting op de totstandkoming van de dataset REGIS II, *Report 05-038-b*, Netherlands Institute of Applies Geosciences TNO.